

Tectonic interpretation of the metamorphic field gradient south of the Koralpe in the Eastern Alps

Alexandra HERG^{*)} & Kurt STÜWE

Institute of Earth Sciences, University of Graz, Universitätsplatz 2, A-8010, Graz, Austria;

^{*)} Corresponding author: Alexandra Herg, alexandra@m-herg.at



KEYWORDS Pohorje; Koralpe; slab extraction; Plattengneis-Plankogel shear zone

Abstract

In order to constrain tectonic models for the nature of the Eoalpine high pressure belt at the eastern end of the Alps, we investigate the formation pressure of metamorphic rocks along a profile between the Koralpe and the well-known UHP rocks of the southern Pohorje mountains. Rocks from three different regions are considered: (i) the rocks of the southernmost Koralpe to the north, (ii) the rocks of the Plankogel Unit between the Plankogel detachment and the Drava valley and (iii) the rocks between the Possruck range and the southern Pohorje mountains. In the Koralpe, pelitic rocks record a formation pressure around 15 – 18 kbar, as reported in the literature. For the Plankogel Unit, we derive pressures between 7.1 ± 1.95 kbar and 11.5 ± 3.42 kbar at 650 °C and recognize only a single Eoalpine metamorphic event. For the high grade rocks of the Pohorje mountains, we derive peak metamorphic pressures (explored with the garnet-muscovite-kyanite-quartz assemblage) that rise from 16.2 ± 3.45 kbar (at 700°C) in the north, to 23.9 ± 2.49 kbar (at 700 °C) in the south. There, we also recognize a later lower pressure event that is derived from pressure calculations with the full equilibrium assemblage. This lower pressure event yields similar conditions around 10 ± 2 kbar at 650 °C for the entire north-south transect within the Pohorje mountains. Peak metamorphic conditions in the Koralpe and Pohorje regions are matched by a continuous field gradient of about 1.3 kbar per 10 kilometers distance corresponding to a depth increase of about 0.5 km per kilometers distance assuming lithostatic conditions. We suggest that this supports that the two units may be interpreted together in terms of a 45° dipping subducting plate. Above this subducting plate, it is inferred that a slab was extracted that was located between the Plankogel Unit and the high pressure rocks, causing a first exhumation stage that is associated with buoyant upwards tilting of the subducted slab to mid crustal levels. Within this model, the Plankogel Unit was located in the hanging wall of the extracted slab and the Plankogel detachment forms the suture of the extracted slab. Exhumation from mid crustal levels to the surface during a 2nd stage occurred due to erosion and normal faulting. This normal faulting is responsible for some 10 km of upward displacement of the Pohorje mountains relative to the Koralpe and ultimately for the current distribution of lithologies on a map scale.

1 Introduction

Slab extraction on an orogenic scale describes the downward removal of a large body of rocks within a subduction zone (Froitzheim et al., 2003, 2006). In the Saualpe-Koralpe-Pohorje regions of the Eastern Alps, this process has been proposed as a mechanism to explain the partial exhumation of high grade metamorphic rocks (e.g. Janák et al., 2009, 2015; De Hoog et al., 2009). There, the southward dipping Plattengneis-Plankogel shear zone (detachment) was recently suggested to be the trace of a slab that was extracted in the context of Eoalpine subduction (Schorn and Stüwe, 2016). This interpretation is consistent with a decrease in formation pressure for the metamorphic parageneses from 23 – 24 kbar to 12 – 14 kbar across the south dipping shear zone (Schorn and Stüwe, 2016), but these authors also recognized some shortcomings of this model. More importantly, however, formation pressure of rocks increases again further south in the Pohorje mountains (up to 40 kbar for garnet peridotites in the Slovenska Bistrica ultramafic complex (Janák et al., 2006; De Hoog et al., 2009)).

The reappearance of high-pressure metamorphic rocks south of the hanging wall of the inferred extraction fault is – at first sight – puzzling (Fig. 1). Indeed, it raises questions about the role of slab extraction in connection with the exhumation of high- and ultrahigh-pressure rocks in the Pohorje area and to what extent the Saualpe, Koralpe and Pohorje regions share a common tectonic history. Answers to this puzzle can be supported by a careful documentation of the metamorphic field gradient across the region.

In this paper, we follow up from studies of the metamorphic pressure in the Koralpe (e.g. Tenczer and Stüwe, 2003) and investigate the metamorphic field gradient in a region where little data exist. This is the region between the well-known Koralpe- and the Pohorje areas. We focus in particular on the formation pressure of the high grade metamorphic parageneses. The results of this documentation support a model that explains the Pohorje and Koralpe regions in terms of a common slab-extraction process.

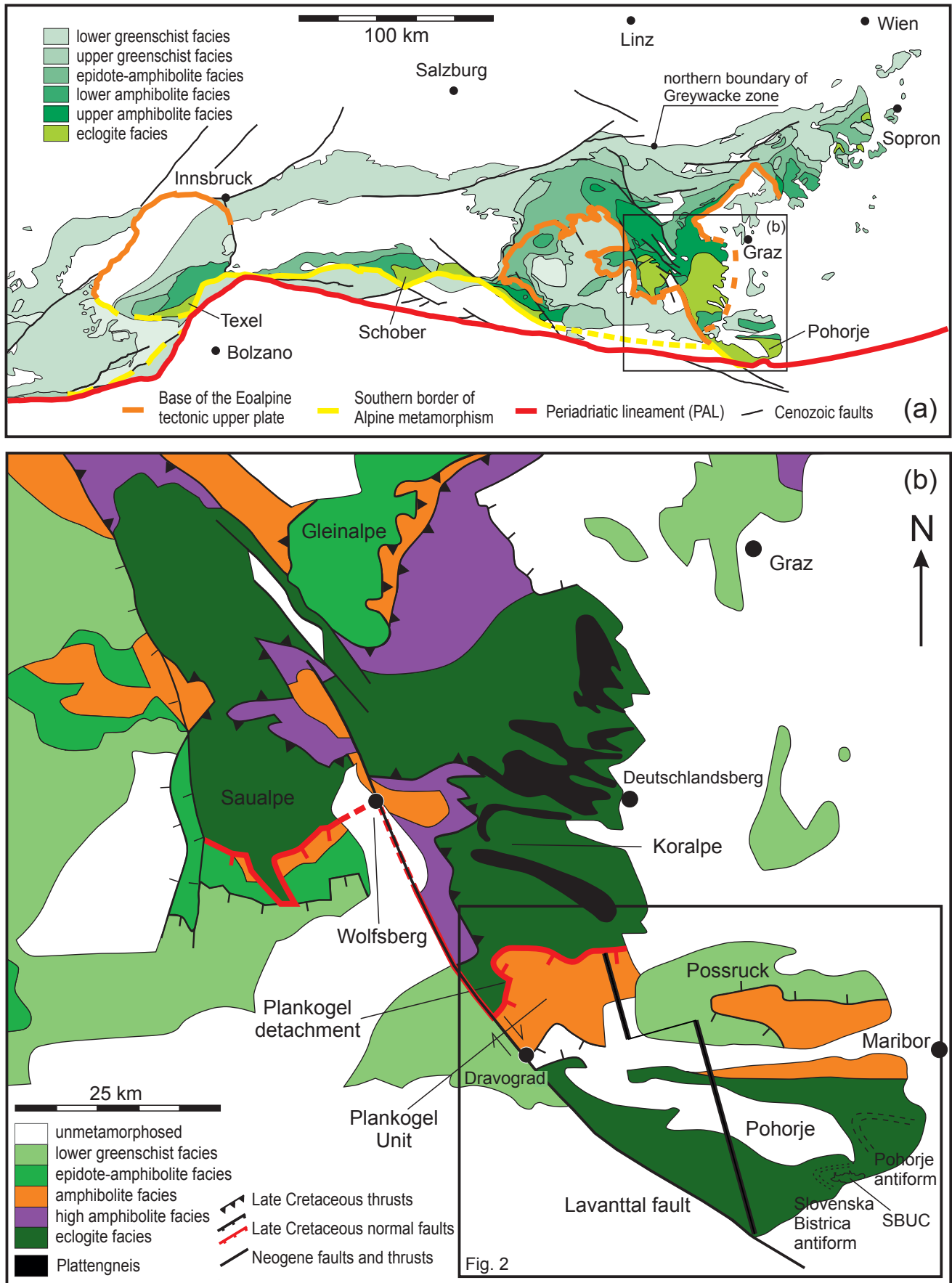


Figure 1: Maps of the location and metamorphic setting of the study area. (a) Simplified metamorphic map of the Eastern Alps (modified after Schuster, 2003). The Eoalpine high pressure belt of the eastern Alps includes the high-grade metamorphic rocks from the Texel group to the Pohorje mountains. (b) Simplified metamorphic map of the Saualpe-Koralpe-Pohorje area showing metamorphic grade (modified after Froitzeim et al., 2008). The line across the Pohorje indicates the transect along which samples were taken. The box indicates position of Fig. 2.

2 Geological setting

Following the closure of the Meliata Ocean in the Jurassic, the continuing north-south convergence between Africa and Europe led to convergence within the Adriatic plate (Stüwe and Schuster, 2010). Around 145 Ma, this led to the initiation of a south- to southeast-dipping, intra-continental subduction zone (Janák et al., 2004; Stüwe and Schuster, 2010). The ongoing subduction led to thrusting and nappe stacking in the northern Adriatic continental block and to high- and ultrahigh-pressure metamorphism (Janák et al., 2004). The high pressures determined for these rocks indicate burial depths of up to 100 km (Janák et al., 2015). The Eoalpine high pressure metamorphic belt is interpreted to be the present day reflection of these dramatic Cretaceous processes (Thöni and Jagoutz, 1993) and the Koralpe-Saualpe-Pohorje regions preserve the most complete record of this geological evolution and its subsequent exhumation history (Fig. 1).

The Pohorje mountains at the southern end of this transect are interpreted to be the most deeply subducted part of the Alps during the Cretaceous orogeny (Janák et al., 2004, 2005, 2006, 2009, 2015; Thöni, 2006; Miller et al., 2007; Kirst et al., 2010). In the Slovenska Bistrica ultramafic complex ("SBUC" after Janák et al., 2006) in the south of the Pohorje mountains, eclogites yield peak metamorphic conditions at 30 – 31 kbar and 760 – 825 °C according to Janák et al. (2004) or 30 – 37 kbar and 710 – 940 °C according to Vrabec et al. (2012), whereas the garnet peridotites may even have suffered 40 kbar at around 900 °C (Janák et al., 2006; De Hoog et al., 2009). Earlier studies, on the other hand, had determined lower conditions at 18 – 25 kbar and 630 – 700 °C (Sassi et al., 2004) and >21 kbar and <750 °C (Miller et al., 2005) for eclogites. Since then, Janák et al. (2015) could verify UHP conditions by investigating diamonds in both, eclogites and gneisses of the SBUC. For metapelites in close vicinity of the SBUC, peak pressure values of 27.5 kbar at 780 °C (Hurai et al., 2010) and 21 – 27 kbar at 700 – 800 °C (Janák et al., 2009) were calculated. The decompression conditions were determined through a lower pressure overprint at about 9 kbar at 720 °C (Hurai et al., 2010) and 5 kbar at 550 °C (Janák et al., 2009). Structurally, the SBUC is interpreted to be the core of an antiformal structure known as the Slovenska Bistrica antiform that formed during the exhumation stage (Kirst et al., 2010) (Figs. 1, 2).

In the Koralpe region at the northern end of the transect, a metamorphic field gradient has been determined in metapelites (Tenczer and Stüwe, 2003). This gradient increases continually in pressure from about 10 kbar in the north to eclogite facies pressures around 17 kbar in the central Koralpe. Eclogites in the region have yielded somewhat higher pressures around 20 kbar at 700 °C (Hoinkes et al., 1999). In the Saualpe to the west of the Koralpe, a similar gradient has been documented but peak pressures are somewhat higher: about 22 kbar and 630–740 °C are documented for the highest grade rocks there (Thöni et al., 2008; Schorn and Stüwe, 2016).

The Plankogel detachment represents the southern, abrupt termination of the eclogite facies peak conditions in both the Koralpe and the Saualpe regions. This detachment is an east-west striking and southward dipping shear zone with top to the south motion, juxtaposing the eclogite facies rocks of the Koralpe towards the amphibolite facies rocks further south (Gregurek et al., 1997; Tenczer and Stüwe et al., 2003; Eberlei et al., 2014). The Plankogel Unit in the immediate hanging wall of the detachment consists of an approximately 400 m thick sequence of mainly garnet-micaschists of substantially lower formation pressures that crops out in the southernmost Koralpe and the Possruck range (Gregurek et al., 1997). Pressures determined for the Cretaceous event in this unit are generally between 7 – 10 kbar with temperatures of 550 – 600 °C and around 5 kbar and 540 °C for an earlier Permian event (Gregurek et al., 1997; Thöni and Miller, 2009).

Between the Plankogel Unit and the Pohorje mountains, the metamorphic field gradient in the high pressure rocks is not well known. This is in part because the investigation of this transect is complicated by the fact that it is interrupted by several different units: In the immediate hanging wall of the Plankogel Unit there are two low grade units of phyllites with minor limestone, interpreted to be part of the Upper Central Austroalpine, i.e. the hanging wall of the Eoalpine subduction zone (Kirst et al., 2010). These units are also found south of the Plankogel Unit in the Saualpe transect (Wiesinger et al., 2006; Neugebauer, 1970). These slates and phyllites are overlain by relicts of unmetamorphosed Permo-Triassic and Senonian sediments (Hinterlechner-Ravnik, 1977) that only crop out in the western end of the region. The metamorphic field gradient in the central part of the transect between Koralpe and Pohorje is obscured by a Miocene batholithic intrusion (Fodor et al., 2008; Trajanova et al., 2008). This intrusion is accompanied by rhyodacitic dykes and thin lamprophyre dykes in the northwest and west of the pluton (Trajanova et al., 2008). Finally, in some regions Miocene sediments cover all of the above described units, in particular in the Ribnica trough south of the Drava valley (Fig. 2).

2.1 Slab extraction in the Koralpe-Pohorje transect

The model of slab extraction for the exhumation of the high pressure rocks described above is based in part on the structural relationships of the different units and in part on the evidence for partial overprinting of the parageneses at lower pressure (Froitzheim et al., 2003; Janák et al., 2004, 2006).

Structurally, the model involves the downward extraction of a mantle and lower crustal wedge overlying the subducted rocks, thus allowing these very deeply subducted rocks to be partially exhumed. The high pressure rocks from both the Koralpe region and the SBUC are interpreted to have been part of the downgoing lower plate below the extracted wedge (Kirst et al., 2010). The timing of this process is constrained by

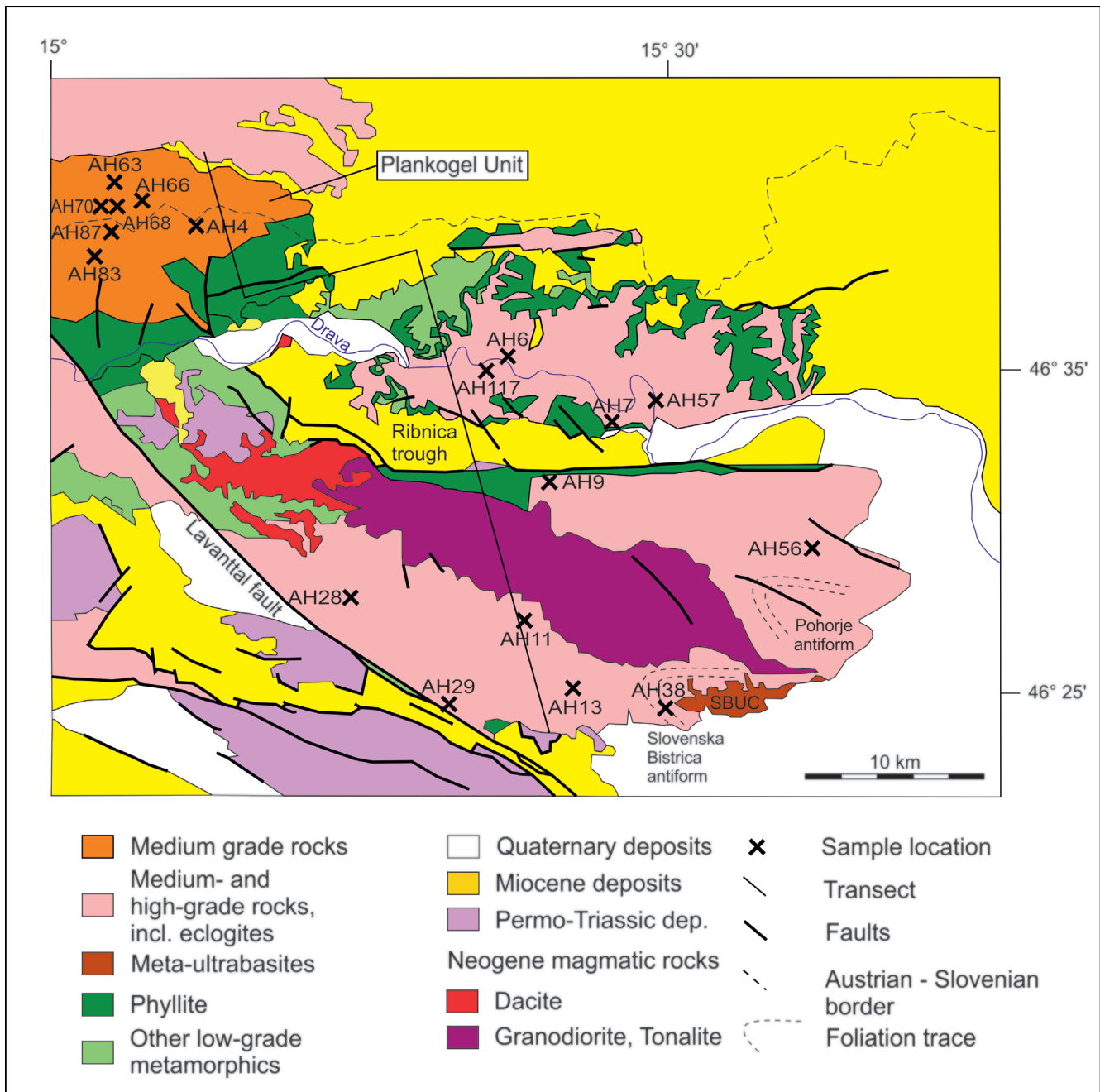


Figure 2: Simplified geological map showing the investigated area (modified after Mioč and Žnidarčič, 1977). The black line represents the transect onto which sample locations are projected. Sample localities are marked within the map.

Lu – Hf garnet chronometry that yields ages from 97 to 90 Ma for eclogites in the SBUC (Sandmann et al., 2016) and by Sm – Nd dating of garnet in metapelites that shows ages of 93 – 87 Ma (Thöni, 2002). These values are similar to the ages of high-pressure metamorphism and cooling ages for the Koralpe and Saualpe (Thöni and Jagoutz, 1992; Thöni and Miller, 1996; Miller and Thöni, 1997; Thöni, 2002), suggesting a common tectonic history during the Eoalpine subduction and exhumation (Janák et al., 2004). Within the slab extraction model, the Plankogel detachment and the Plattengneis shear zone of the Koralpe are interpreted to be both part of the same shear zone system (“PGPK shear zone” after Schorn and Stüwe, 2016) and to represent the suture of

the downwards extracted slab (Schorn and Stüwe, 2016; Eberlei et al., 2014).

Petrologically, this model is supported by observations that record an amphibolite facies overprint over the eclogite facies parageneses suggesting a hiatus in the exhumation history. This hiatus in the eclogite facies rocks of the Saualpe, Koralpe and the Pohorje regions is suggested to have occurred when the lower plate was joined with the upper plate following the downward extraction of the slab, but prior to final exhumation. Conversely, in the amphibolite facies rocks of the Plankogel Unit, this overprint is notably absent (Schorn and Stüwe, 2016). The final exhumation of the entire transect to the surface occurred by erosion driven exhumation in the uppermost

Cretaceous and the Paleogene (e.g. Neubauer, 1995) and through east- to north-east-directed low-angle extensional shearing during the Early to Middle Miocene (Fodor et al., 2002).

3 Petrography and mineral chemistry

For the purpose of this study, some 120 samples were collected from high grade metamorphic rocks in the southern Koralpe, Plankogel and northern Pohorje regions to cover a north-south profile as shown in Figs. 1 and 2. The low grade phyllites were not sampled. Amphibolites, eclogites, strongly weathered samples, and samples which appeared to have a lack of petrologically useful phases were neglected and 43 thin sections of metapelitic gneisses were cut. The thin-sections were analyzed under a polarizing microscope and a subset of 20 samples was chosen for further analyses with the electron microscope and geothermobarometric calculations. Mineral chemical analyses were carried out using a JEOL JSM-6310 scanning electron microscope equipped with a Link ISIS EDX-System and Microspec WDX-600i system at the Institute of Earth Sciences, University of Graz, Austria. Measurements were performed on polished, carbon-coated thin-sections with measurement conditions of 15 kV acceleration voltage and 6 nA beam current. Representative mineral analyses are shown in Tabs. 1 and 2. Mineral abbreviations are according to THERMOCALC (Holland and Powell, 1998) and we note that THERMOCALC terms all white mica as "muscovite". The results were spatially projected onto a profile from northwest to southeast as shown on Fig. 2.

3.1 Pelitic rocks of the Koralpe

Pelitic rocks in the Koralpe region north of the Plankogel detachment have been well-described in the literature (e.g. Gregurek et al., 1997; Tenczer and Stüwe, 2003; Miller and Thöni, 1997 and references therein) and this information is only briefly summarized here. The typical assemblage includes garnet, white mica, biotite, plagioclase and quartz, together with or without kyanite (e.g. Eberlei et al., 2014). In the Plattengneis, potassium feldspar is also abundant, but it is usually mantled by thin seams of plagioclase or quartz and is inferred to be related to deformed Permian pegmatite remnants and not part of the Eoalpine equilibrium assemblage (Tenczer et al., 2006). Garnet porphyroblasts are present in all assemblages of the pelitic rocks and are rich in inclusions (Gregurek et al., 1997; Tenczer and Stüwe, 2003). Larger garnets typically have Permian cores and Eoalpine rims (e.g. Schuster and Stüwe, 2008; Thöni and Miller, 2009). Garnets within the gneisses are partly boudinaged and often surrounded by biotite (Kurz et al., 2002). White mica is often seen to be mantled by biotite (Eberlei et al., 2014). In the footwall rocks of the Plattengneis shear zone, staurolite is occasionally present and may appear as coarse grains, in particular in the southern parts of the Koralpe region (Tenczer and Stüwe, 2003). Kyanite occurs commonly as elongated aggregates often pseudomorphing

Permian andalusite (Tenczer and Stüwe, 2003; Schuster and Stüwe, 2010).

3.2 Pelitic rocks of the Plankogel Unit

Garnet-micaschists of the Plankogel Unit are often characterized by large garnet porphyroblasts (Kleinschmidt, 1975). The matrix is made up of quartz, white mica and biotite. The paragenesis of the Plankogel rocks is largely identical to the those in the Koralpe, but it formed at lower pressure which is – in part – evidenced by the fact that staurolite is part of the inferred peak paragenesis (Schorn and Stüwe, 2016).

Garnet forms porphyroblasts with diameters of up to 1 cm (Fig. 3a, b, c). Most of them also exhibit some sort of compositional or textural zoning (Fig. 3). X_{Fe} (= molar Fe/(Fe + Mg)) varies in zoned garnets between 0.91 and 0.96 whereas X_{Ca} (= molar Ca/(Ca + Fe + Mg)) ranges from 0.12 at the rim to 0.03 towards the core. Some garnet cores still preserve relics of the Permian metamorphic event (Thöni and Miller, 2009). Representative mineral analyses of a zoned garnet are shown in the supplementary material Tab. S1. Inclusions of quartz, biotite, white mica, chlorite, chloritoid and staurolite occasionally occur within garnets.

White mica can be found throughout all thin-sections occurring either as mica fish, as smaller grains distributed within the matrix or as inclusion in garnets. In some samples, it is characterized by very small grains making up a fine matrix. Mineral analyses show that white mica in the Plankogel Unit is typically muscovite. Biotite occurs in most samples as fine grains within the matrix or as inclusions in garnet. It also occurs in association with chlorite on the outside of larger garnet grains.

Plagioclase is only present in small amounts in sample AH4 (Fig. 3e). Small grains of plagioclase can be found within the quartz-dominated matrix. Staurolite is common in most samples of the Plankogel Unit. It appears in several thin-sections in the shape of subhedral elongated grains with up to 3 mm length. They were found within the matrix or as inclusions within a garnet. Zoisite was found only in sample AH4 in the shape of needles following the orientation of the foliation (Fig. 3f).

Chloritoid occurs only in samples AH87 and AH83 either as inclusion within a garnet or in the matrix. Grains are euhedral and up to almost 1 mm in length. Chlorite is present in most samples within the matrix or as inclusion in garnets. Late chlorite rimming garnet and biotite was also found. Kyanite is only found in sample AH63 as small grains within the matrix (Fig. 3d). Accessories are mostly rutile, epidote and opaque phases such as ilmenite. The inferred equilibrium assemblage used for pressure calculations is garnet + muscovite + biotite ± plagioclase ± staurolite ± zoisite ± chloritoid ± chlorite + (kyanite + quartz + H₂O).

3.3 Pelitic rocks of the Pohorje region

The metapelites of the Pohorje region include not only high metamorphic grade gneisses, but also phyllitic

Sample Phase Position Label	AH83		AH87		AH83		AH87		AH83		AH87		AH83		AH87	
	Garnet		Muscovite		Biotite		Chlorite		Staurolite		Chloritoid		AH83		AH87	
	rim	matrix	rim	matrix	rim	matrix	rim	matrix	rim	matrix	rim	matrix	rim	matrix	rim	matrix
SiO ₂	37.88	36.97	48.78	47.07	37.23	26.56	26.66	26.07	28.57	28.62	25.31	24.38				
TiO ₂	0.01	0.02	0.39	0.36	1.41	0.13	0.15	0.10	0.38	0.58	0.01	0.03				
Al ₂ O ₃	21.11	21.25	38.21	35.75	20.03	23.96	24.01	24.33	56.72	53.02	42.67	40.01				
Cr ₂ O ₃	0.06	0.00	0.03	0.01	0.00	0.12	0.00	0.02	0.04	0.00	0.00	0.00				
Fe ₂ O ₃	0.00	1.11	0.00	0.00	0.00	3.87	0.00	0.00	0.00	0.00	0.00	0.00				
FeO	37.08	30.93	0.96	0.93	19.59	19.71	24.64	22.61	14.54	14.18	23.38	21.35				
MnO	0.73	0.04	0.01	0.00	0.02	0.00	0.00	0.00	0.03	0.05	0.09	0.00				
MgO	1.93	3.49	0.27	0.37	10.52	17.84	14.23	18.25	2.01	2.27	3.20	4.12				
CaO	2.15	5.42	0.01	0.00	0.01	0.00	0.03	0.00	0.02	0.03	0.00	0.00				
Na ₂ O	0.00	0.00	1.87	1.78	0.29	0.00	0.03	0.02	0.00	0.00	0.00	0.00				
K ₂ O	0.04	0.03	8.62	8.75	9.07	0.03	0.25	0.02	0.03	0.00	0.03	0.00				
Total	100.99	99.26	99.15	95.01	98.18	92.22	90.02	91.41	102.34	98.75	94.70	89.89				
Oxygen	12.0	12.0	11.0	11.0	11.0	11.0	14.0	14.0	46.0	46.0	6.0	6.0				
Si	3.030	2.963	3.079	3.109	2.727	2.039	2.704	2.580	7.584	7.875	1.009	1.019				
Ti	0.001	0.001	0.019	0.018	0.078	0.008	0.012	0.007	0.075	0.120	0.000	0.001				
Al	1.991	2.008	2.843	2.784	1.730	2.168	2.871	2.838	17.750	17.198	2.005	1.971				
Cr	0.004	0.000	0.001	0.001	0.000	0.007	0.000	0.002	0.009	0.000	0.000	0.000				
Fe ³⁺	0.000	0.067	0.000	0.000	0.000	0.223	0.000	0.000	0.000	0.000	0.000	0.000				
Fe ²⁺	2.481	2.073	0.051	0.051	1.200	1.265	2.090	1.871	3.228	3.262	0.779	0.746				
Mn	0.050	0.003	0.001	0.000	0.001	0.000	0.000	0.000	0.008	0.012	0.003	0.000				
Mg	0.230	0.417	0.025	0.037	1.148	2.041	2.151	2.691	0.794	0.930	0.190	0.257				
Ca	0.184	0.465	0.001	0.000	0.001	0.000	0.003	0.000	0.006	0.007	0.000	0.000				
Na	0.000	0.000	0.228	0.228	0.041	0.000	0.006	0.003	0.000	0.002	0.000	0.000				
K	0.004	0.003	0.694	0.737	0.848	0.003	0.033	0.003	0.010	0.000	0.002	0.000				
Total	7.974	8.000	6.942	6.964	7.775	7.755	9.869	9.996	29.466	29.407	3.989	3.994				

Table 1: Representative mineral compositions for samples of the Plankogel Unit. Both cations and oxide formulas are recalculated from measured oxides using AX.

Sample Phase Position Label	AH7	AH11	AH7	AH11	AH7	AH11	AH7	AH11	AH7	AH11
	Garnet		Muscovite		Biotite		Chlorite		Plagioclase	
	matrix	matrix	matrix	matrix	matrix	matrix	matrix	matrix	matrix	matrix
	ah7_1_11	ah11_2_1	ah7_1_17	ah11_1_25	ah7_1_18	ah11_5_18	ah7_2_7	ah11_7_10	ah7_4_2	ah11_7_6
SiO ₂	38.33	37.58	48.08	47.99	36.43	34.53	25.87	25.12	64.88	38.94
TiO ₂	0.01	0.00	1.09	0.91	1.71	1.58	0.05	0.04	0.07	0.06
Al ₂ O ₃	21.31	20.73	32.32	31.38	16.64	17.33	20.40	20.92	23.39	31.64
Cr ₂ O ₃	0.10	0.04	0.06	0.06	0.09	0.02	0.04	0.00	0.01	0.08
Fe ₂ O ₃	1.60	1.31	0.00	0.00	0.00	1.83	0.00	0.00	0.00	1.13
FeO	25.70	24.78	1.68	1.60	18.73	17.89	29.82	24.38	0.00	0.00
MnO	0.63	0.49	0.00	0.01	0.12	0.16	0.24	0.32	0.00	0.09
MgO	3.99	5.52	1.83	2.17	10.87	10.26	11.55	15.22	0.00	0.07
CaO	9.54	7.55	0.00	0.00	0.04	0.08	0.06	0.02	4.27	23.02
Na ₂ O	0.04	0.03	0.81	0.65	0.09	0.14	0.00	0.03	9.31	0.08
K ₂ O	0.00	0.00	10.32	9.60	9.55	8.45	0.05	0.00	0.11	0.03
Total	101.24	98.04	96.20	94.37	94.27	92.29	88.09	86.06	102.03	95.13
Oxygen	12.0	12.0	11.0	11.0	11.0	11.0	14.0	14.0	8.0	8.0
Si	2.977	2.990	3.176	3.214	2.800	2.709	2.777	2.690	2.807	1.944
Ti	0.000	0.000	0.054	0.046	0.099	0.093	0.004	0.004	0.002	0.002
Al	1.951	1.944	2.517	2.478	1.508	1.603	2.582	2.642	1.193	1.862
Cr	0.006	0.003	0.003	0.003	0.005	0.001	0.004	0.000	0.000	0.003
Fe ³⁺	0.094	0.079	0.000	0.000	0.000	0.108	0.000	0.000	0.000	0.042
Fe ²⁺	1.669	1.649	0.093	0.090	1.204	1.174	2.677	2.184	0.000	0.000
Mn	0.041	0.033	0.000	0.000	0.008	0.011	0.021	0.029	0.000	0.004
Mg	0.462	0.655	0.180	0.216	1.245	1.200	1.847	2.429	0.000	0.005
Ca	0.794	0.643	0.000	0.000	0.003	0.007	0.007	0.003	0.198	1.231
Na	0.006	0.005	0.104	0.085	0.013	0.022	0.000	0.007	0.781	0.008
K	0.000	0.000	0.870	0.820	0.936	0.846	0.007	0.000	0.006	0.002
Total	8.000	8.000	6.997	6.953	7.821	7.776	9.929	9.988	4.987	5.104

Table 2: Representative mineral compositions for samples of the Pohorje mountains. Both cations and oxide formulas are recalculated from measured oxides using AX.

units. However, here we focus only on the high grade rocks (Fig. 2). These are mainly coarse-grained gneisses and micaschists with a similar assemblage. They are commonly foliated and show a general mineralogical composition of quartz + garnet + white mica + biotite ± plagioclase ± staurolite ± zoisite ± chloritoid ± chlorite ± kyanite (Fig. 4).

Garnet grains are mostly subhedral and slightly fractured. Samples in the Pohorje region include significantly smaller specimens than in both, the Koralpe and the Plankogel rocks with less obvious optical or compositional zoning. Inclusions of quartz, biotite, white mica and chlorite occasionally occur within the garnets (Fig. 4a-f).

White mica can be found throughout all thin-sections in varying quantity. White mica occurs either as big mica fish, as smaller grains distributed within the matrix or as inclusion in garnets (Fig. 4d, e). Mineral analyses show various compositions for the white micas in different samples. Al₂O₃ ranges around 30-34 wt%, MgO varies around 0.5 to 2.5 wt%, Na₂O lies typically between 0.5 and 2 wt% and K₂O ranges around 8.5-11 wt%. It can be concluded that most samples in the Pohorje region are phengitic white micas. Mineral analyses are shown in Tabs. 1 and 2. Biotite occurs in most samples as subhedral elongated grains within the matrix or as inclusions in garnet.

Plagioclase was only found in some thin-sections and always in relatively small amounts within the matrix

(Fig. 4c). Staurolite appears occasionally as small grains within the matrix (Fig. 4f). Staurolite is rare in samples collected from the Pohorje mountains.

Chlorite is found in most samples within the matrix or as inclusion in garnets. Chlorite also occasionally appears to be of secondary nature, for example, on the edge of biotite grains. Kyanite is only sporadically present within the examined thin-sections and can be found as small grains within the matrix in samples AH29 and AH56. Accessories are mostly rutile, late epidote and opaque phases such as ilmenite. The inferred equilibrium assemblage is garnet + muscovite + biotite ± plagioclase ± staurolite ± zoisite ± chloritoid ± chlorite + (kyanite + quartz + H₂O).

4 Geothermobarometry

Chemical compositions of minerals of the inferred equilibrium parageneses were recalculated with the program AX (<http://www.esc.cam.ac.uk/research/research-groups/research-projects/tim-hollands-software-pages/ax>) in order to obtain end-member activities. Water is assumed to be in excess in all samples. Geothermobarometry was then performed using THERMOCALC version 3.33 (<http://www.metamorph.geo.uni-mainz.de/thermocalc>; Powell and Holland, 1988) and the internally-consistent thermodynamic dataset of Holland and Powell (1998). Calculations were performed with the average *P-T* method (mode 2), as well as the average *P*

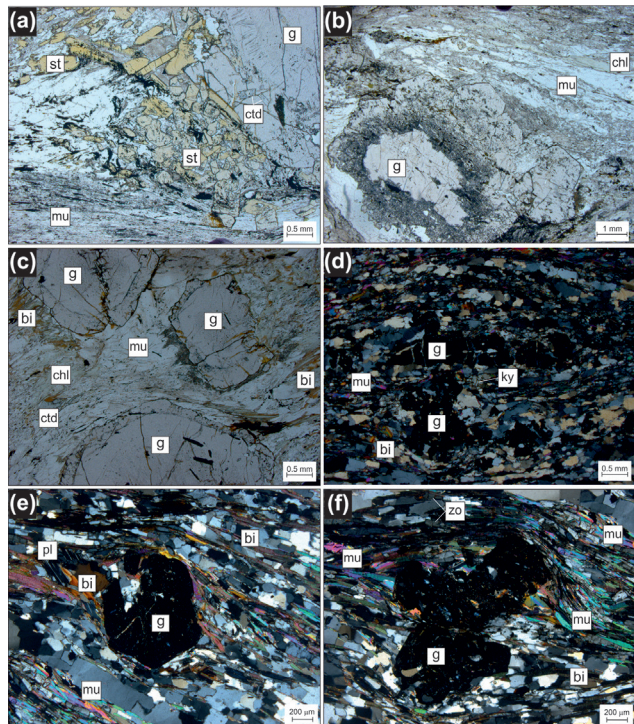


Figure 3: Photomicrographs of representative samples taken from the Plankogel Unit (mineral abbreviations are those used by THERMOCALC, Powell and Holland, 1988). (a)-(c) are shown under parallel polarizing filters and (d)-(f) are shown under crossed polarizing filters. (a) Sample AH87: Garnet-micaschist displaying a zoned garnet porphyroblast with inclusions of chloritoid and staurolite. The matrix is characterized by fine-grained muscovite and quartz including a lot of staurolite. (b) Sample AH68: Large garnet porphyroblast with visible zoning within a matrix of muscovite, quartz and secondary chlorite. (c) Sample AH83: Several garnet porphyroblasts exhibiting visual zoning within a matrix of muscovite, quartz, biotite and secondary chlorite. (d) Sample AH70: Several garnets within a matrix of quartz, muscovite and biotite. Note the kyanite in between the garnet grains. (e) and (f) Sample AH4: Garnet-micaschist showing several garnet porphyroblasts. (e) shows a plagioclase next to the garnet whereas (f) displays several needles of zoisite alongside muscovite surrounding the garnet.

method (rock calculations type 1) of Powell and Holland (1994). After setting either a temperature window or a fixed temperature, pressure values are calculated for the desired conditions. The output pressures are given with a corresponding error margin and sigfit value. The sigfit value shows the quality of how well selected end-member activities match among one another (Powell and Holland, 1994). The smaller the sigfit value the more accurate and reliable the result. Different combinations of mineral analyses were tested for each individual sample in order to keep the error margin and sigfit values as low as possible and achieve reliable results.

In view of our aim to derive peak formation pressure for the metamorphic parageneses it is important to note that Janák et al. (2009) performed calculations of formation conditions for metapelites in the immediate surroundings of the SBUC and argued that pressures calculated with the full assemblage reflect an equilibration event at lower pressure and not the peak pressure metamorphic conditions. They derived the peak pressure conditions by using only garnet cores + phengitic white

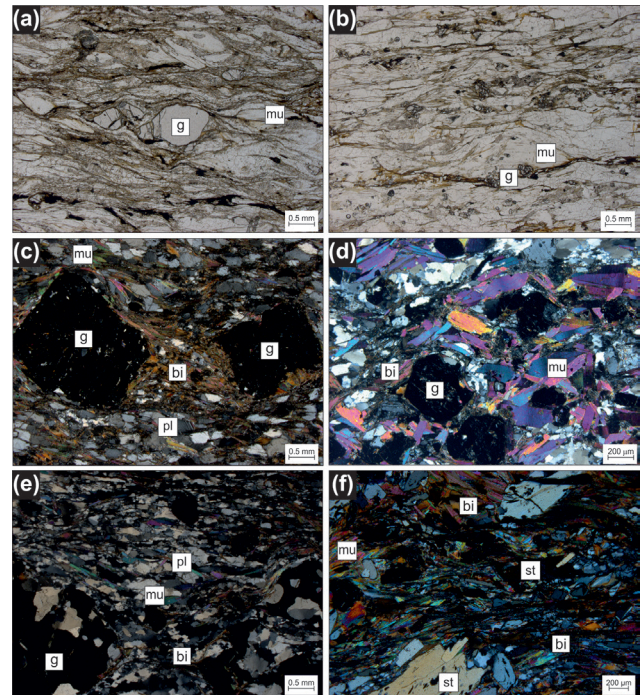


Figure 4: Photomicrographs of representative samples taken from the Pohorje region (mineral abbreviations are those used by THERMOCALC, Powell and Holland, 1988). (a) and (b) are shown under parallel polarizing filters and (c)-(f) are shown under crossed polarizing filters. (a) Sample AH11: Small garnet porphyroblasts within a matrix of mainly quartz. Large mica fish are present within the thin-section. (b) Sample AH13: Garnet is only sporadically present within a matrix of quartz and muscovite. (c) Sample AH6: Large garnet porphyroblasts within a matrix of quartz, biotite and muscovite which also occasionally displays plagioclase. (d) Sample AH7: Garnets and large mica fish are found within a matrix of quartz. (e) Sample AH29: Fine-grained matrix includes garnet porphyroblasts and sporadic plagioclase. (f) Sample AH56: Fine-grained matrix of mainly muscovite and biotite contains small garnet and large staurolite porphyroblasts.

mica + kyanite + quartz. This method yielded significantly higher pressures which are, however, still considered as minima due to the possibility of diffusion-related modification of the garnet composition at high temperatures and the re-equilibration of phengite during early stages of decompression (Janák et al., 2009).

4.1 Geothermobarometric results

In view of the suggestion by Janák et al. (2009), two sets of barometric calculations were performed for each sample: (a) for the complete Eoalpine equilibrium assemblage as described above and (b) for the assemblage $g + mu + ky + q$, which may be useful to extract the highest pressures the rocks experienced during Eoalpine metamorphism. In this context, the reader is reminded that the Eoalpine equilibrium assemblage differs between the rocks in the Pohorje region and those of the Plankogel Unit. In the Pohorje rocks, the Eoalpine event is interpreted to have overprinted all relics of a Permian event (Janák et al., 2009) so that the Eoalpine equilibrium assemblage is the complete assemblage reported above and garnet cores can be used as part of this paragenesis (Tab. 3). In contrast, the rocks from the Plankogel Unit (samples AH4, AH63, AH68, AH66, AH70, AH83 and AH87) still preserve

relics of the Permian metamorphic event in garnet cores (Thöni and Miller, 2009). Therefore, pressures for the Plankogel Unit were determined by using chemical data from the garnet rims and the rest of the assemblage.

Using the complete Eoalpine equilibrium assemblage, calculations yield pressure values around 10 kbar for all analyzed samples from both the Plankogel Unit and the Pohorje mountains (Fig. 5; Tab. 4a). The lowest obtained value is 7.1 ± 1.95 kbar, whereas the highest value is 12.9 ± 1.82 kbar with this range being similar for both the Plankogel Unit and the Pohorje mountains. Most pressures range between 9 and 11 kbar. The best method to achieve pressure values as accurate as possible proved to be to change temperature conditions within THERMOCALC and to repeatedly replace individual measurements of the same mineral with each other. For the re-equilibrated conditions, it worked best to use measurements of minerals in close proximity to each other. Pressures were iteratively calculated for a series of temperatures, but the results given here are for 650 °C which gave the smallest error bars on the pressures and is also consistent with the temperatures for a late stage equilibration event along the decompression path suggested by Janák et al. (2009), Janák et al. (2015), Schorn and Stüwe (2016) or Hurai et al. (2010).

Using only the assemblage of $g + mu + ky + q$, significantly higher pressures were obtained for some rocks, in particular those in the Pohorje mountains (Fig. 5; Tab. 4b). Best results were obtained for an assumed formation temperature of 700 °C. Some samples did not yield any results by using the assemblage of $g + mu + ky + q$ which explains the smaller amount of results for peak metamorphic conditions (Fig. 5). Kyanite is only present in a few thin-sections. For the Plankogel Unit, PT calculations with this reduced assemblage yield similar results to the conditions reported above. However, for the Pohorje rocks, the error margin increased due to the smaller amounts

of data entered into the program. Nevertheless, sigfit values decrease, giving well-constrained results (Tab. 4). Thus obtained peak pressures seem to rise throughout the Pohorje mountains, starting with 16.2 ± 3.45 kbar in the north and rising to a maximum of 23.9 ± 2.49 kbar in the south. In between, pressures range from 18 to 22 kbar only to drop slightly again for the southernmost samples to 17.5 ± 4.06 kbar.

5 Discussion

The barometric data presented above may be interpreted in terms of a metamorphic field gradient if the derived pressures along the transect can be related to the same metamorphic event. For the Plankogel Unit, it can be assumed that the calculated formation pressures correspond to the Cretaceous peak conditions since the Plankogel Unit does not exhibit significant signs of a post Eoalpine re-equilibration event and Permian relics were avoided during the analyses. In contrast, the rocks from the Pohorje region contain no Permian relics and the highest obtained pressures are interpreted to be related to the Eoalpine peak. Similarly, in the Koralpe, highest pressures derived by Tenczer and Stüwe (2003) are inferred to be the Cretaceous Eoalpine peak. Hence, the pressures derived for the Plankogel Unit can be compared with the highest obtained pressure values from the Pohorje and Koralpe regions in terms of a metamorphic field gradient.

The derived formation pressure conditions yield an interesting peak metamorphic field gradient for the study area (Fig. 5). In summary from above, pressures in the Plankogel Unit including the calculated error margin range from 5.15 kbar to 14.92 kbar and only two samples yield values above 13 kbar. In the Pohorje mountains, peak pressures are generally higher and values from 13.05 kbar to 26.39 kbar were derived. The pressure data from the Pohorje may be fitted by a field

Sample	Assemblage	Reactions
AH68	$g + mu + bi + chl + st$ (+ $q + ky + H_2O$)	$12ames + 5alm + 9q = 8clin + 3daph + 2mst$ $3mst + 4alm = 3fst + 4py$
		$105ames + 55alm + 180ky = 52clin + 33daph + 40mst$ $48ames + 55fst + 20py + 36q = 44daph + 63mst$
		$297clin + 40fst = 32daph + 195ames + 235py + 360H_2O$ $17ames + 10east + 39q = 16clin + 2mst + 10mu$
AH70	$g + mu + bi + st$ (+ $q + ky + H_2O$)	$3mst + 4alm = 3fst + 4py$ $2ann + mu + 6q = 3fcel + alm$
		$3east + 6q = phl + 2mu + py$ $2fst + 31fcel = 13ann + 18mu + 46q + 4H_2O$
		$31phl + 6mst = 24east + 7mu + 23py + 12H_2O$ $phl + east + 6q = 2cel + py$
		$2phl + mu + 2ky = 3east + 5q$
AH66	$g + mu + st$ (+ $q + ky + H_2O$)	$4py + 3fst = 4alm + 3mst$ $39cel + 4fst = 13py + 23mu + 16fcel + 14q + 8H_2O$
		$3cel + 4ky = py + 3mu + 4q$ $8mu + 2mst + 19q = 8cel + 4H_2O + 26ky$
AH87	$g + mu + chl + st + ctd$ (+ $q + ky + H_2O$)	$17clin + 8mst = 3ames + 72mctd + 11py$ $39fctd + 4alm = 7daph + 4fst + 3H_2O$
		$5ames + py + 4q = 3clin + 8mctd$ $17daph + 8fst + 6ky = 84fctd + 11alm$
		$ames + 2ky = 4mctd$ $14daph + 3fcel + 8fst = 3mu + 72fctd + 11alm$
		$39mctd + 4py = 7clin + 4mst + 3H_2O$ $ames + cel = clin + mu$
		$19daph + 10fst + 3q = 96fctd + 13alm$

Table 3: End-member reactions used for barometric calculations. The phases in brackets are assumed to be in excess. Mineral abbreviations are according to THERMOCALC.

Sample	Assemblage	Reactions
AH83	g + mu + bi + chl + st + ctd (+ q + ky + H ₂ O)	$39\text{mctd} + 4\text{py} = 4\text{mst} + 7\text{clin} + 3\text{H}_2\text{O}$ $6\text{mst} + 19\text{ames} + 17\text{q} = 88\text{mctd} + 4\text{py}$ $\text{ames} + 2\text{ky} = 4\text{mctd}$ $2\text{mst} + 13\text{ames} + 11\text{q} = 40\text{mctd} + 4\text{clin}$ $4\text{daph} + 26\text{ky} = 12\text{fctd} + 2\text{fst} + 11\text{q}$ $3\text{daph} + 10\text{ky} = 12\text{fctd} + \text{alm} + 4\text{q}$
AH4	g + bi + ep + fsp (+ q + ky + H ₂ O)	$\text{gr} + \text{q} + 2\text{ky} = 3\text{an}$ $2\text{cz} + \text{q} + \text{ky} = 4\text{an} + \text{H}_2\text{O}$
AH117	g + mu + bi + chl + st (+ q + ky + H ₂ O)	$4\text{py} + 3\text{ames} + 44\text{ky} = 6\text{mst} + 17\text{q}$ $15\text{cel} + 4\text{mst} + 6\text{phl} = 13\text{py} + 21\text{mu} + 2\text{clin}$ $21\text{cel} + 4\text{mst} + 6\text{east} = 13\text{py} + 27\text{mu} + 2\text{clin}$ $5\text{py} + 12\text{mu} + \text{clin} + 9\text{q} = 12\text{cel} + 2\text{mst}$ $11\text{py} + 21\text{mu} + 4\text{clin} + 36\text{ky} = 21\text{cel} + 8\text{mst}$
AH6	g + mu + bi + fsp (+ q + ky + H ₂ O)	$\text{gr} + \text{q} + 2\text{ky} = 3\text{an}$ $3\text{east} + 6\text{q} = \text{py} + \text{phl} + 2\text{mu}$ $\text{phl} + \text{east} + 6\text{q} = \text{py} + 2\text{cel}$
AH7	g + mu + bi + chl + fsp (+ q + ky + H ₂ O)	$3\text{east} + 6\text{q} = \text{py} + \text{phl} + 2\text{mu}$ $3\text{phl} + 4\text{ky} = \text{py} + 3\text{east} + 4\text{q}$ $2\text{east} + \text{ames} + 6\text{q} = \text{py} + 2\text{mu} + \text{clin}$ $\text{cel} + 2\text{clin} + 2\text{ky} = \text{phl} + 2\text{ames} + 5\text{q}$ $2\text{ann} + \text{mu} + 6\text{q} = \text{alm} + 3\text{fcel}$
AH9	g + mu + bi (+ q + ky + H ₂ O)	$3\text{east} + 6\text{q} = \text{phl} + 2\text{mu} + \text{py}$ $2\text{phl} + \text{mu} + 2\text{ky} = 3\text{east} + 5\text{q}$ $\text{phl} + \text{east} + 6\text{q} = 2\text{cel} + \text{py}$
AH11	g + mu + bi + chl + fsp (+ q + ky + H ₂ O)	$\text{gr} + \text{q} + 2\text{ky} = 3\text{an}$ $\text{py} + 2\text{gr} + 3\text{ames} + 6\text{q} = 3\text{clin} + 6\text{an}$ $3\text{ames} + 24\text{an} = 4\text{py} + 8\text{gr} + 12\text{H}_2\text{O} + 18\text{ky}$ $3\text{east} + 6\text{q} = \text{py} + \text{phl} + 2\text{mu}$ $2\text{phl} + 3\text{ames} + 6\text{q} = \text{py} + 3\text{clin} + 2\text{mu}$
AH29	g + mu + bi (+ q + ky + H ₂ O)	$3\text{east} + 6\text{q} = \text{py} + \text{phl} + 2\text{mu}$ $\text{phl} + \text{east} + 6\text{q} = \text{py} + 2\text{cel}$ $3\text{phl} + 4\text{ky} = \text{py} + 3\text{east} + 4\text{q}$
AH56	g + mu + bi + st (+ q + ky + H ₂ O)	$3\text{mst} + 4\text{alm} = 3\text{fst} + 4\text{py}$ $3\text{east} + 6\text{q} = \text{phl} + 2\text{mu} + \text{py}$ $2\text{phl} + \text{mu} + 2\text{ky} = 3\text{east} + 5\text{q}$
AH13	g + mu + bi (+ q + ky + H ₂ O)	$\text{mu} + 2\text{phl} + 6\text{q} = \text{py} + 3\text{cel}$ $2\text{east} + 6\text{q} = \text{py} + \text{mu} + \text{cel}$ $3\text{cel} + 4\text{ky} = \text{py} + 3\text{mu} + 4\text{q}$
AH38	g + mu + bi + st (+ q + ky + H ₂ O)	$3\text{east} + 6\text{q} = \text{py} + 2\text{mu} + \text{phl}$ $6\text{mst} + 31\text{phl} = 23\text{py} + 7\text{mu} + 24\text{east} + 12\text{H}_2\text{O}$ $\text{phl} + \text{q} + 2\text{ky} = \text{py} + \text{mu}$
AH63	g + mu + bi (+ q + ky + H ₂ O)	$3\text{east} + 6\text{q} = \text{py} + \text{phl} + 2\text{mu}$ $\text{phl} + \text{east} + 6\text{q} = \text{py} + 2\text{cel}$ $3\text{phl} + 4\text{ky} = \text{py} + 3\text{east} + 4\text{q}$
AH57	g + mu + bi + fsp (+ q + ky + H ₂ O)	$\text{gr} + \text{q} + 2\text{ky} = 3\text{an}$ $\text{gr} + 2\text{pa} + 3\text{q} = 3\text{an} + 2\text{ab} + 2\text{H}_2\text{O}$ $\text{phl} + \text{east} + 6\text{q} = \text{py} + 2\text{cel}$ $2\text{phl} + \text{mu} + 6\text{q} = \text{py} + 3\text{cel}$

Table 3: Continued.

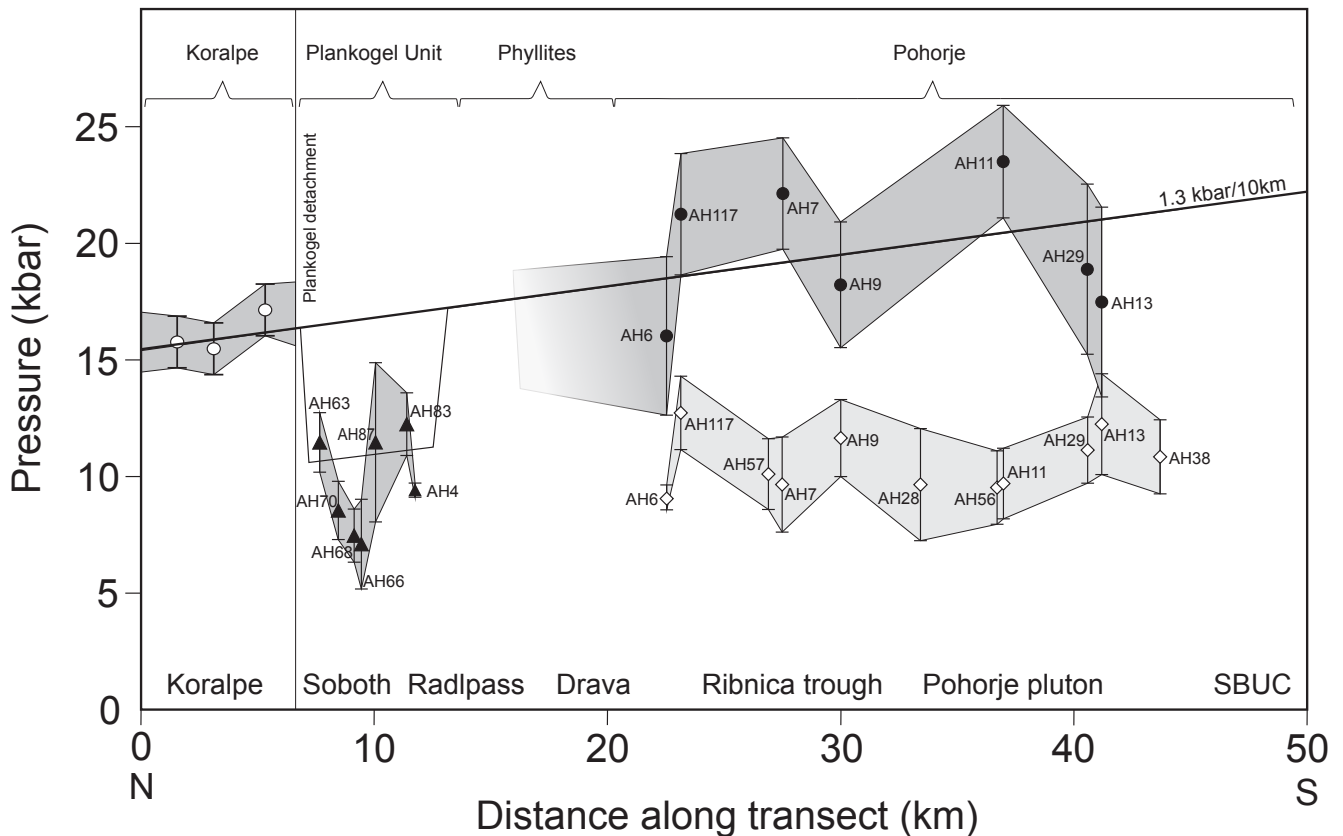


Figure 5: Visual representation of pressure results determined with THERMOCALC along the profile shown in Figs. 1 and 2. The black triangles represent the Plankogel Unit, the black circles represent the peak metamorphic conditions of rocks in the Pohorje area, the white squares represent the decompression conditions of the Pohorje area and the white circles show pressures determined by Tenczer and Stüwe (2003). The transect starts in the Koralpe to the north and ends in the south where the Pohorje mountains dip below the sediments of the Pannonian Basin. The darker shaded area shows the rising pressures from north to south and the lighter shaded area represents the re-equilibrated pressures. The line fitting the peak metamorphic conditions represents the interpreted field gradient discussed in section 5.

(a)

Sample	P (kbar)	sd (kbar)	sigfit	Sample	P (kbar)	sd (kbar)	sigfit
AH63	11.5	1.36	1.0	AH7	9.7	2.00	3.7
AH68	7.5	1.11	1.0	AH57	10.1	1.55	2.9
AH70	8.8	1.21	0.9	AH9	11.7	1.73	1.3
AH66	7.1	1.95	0.8	AH28	9.7	2.54	0.8
AH87	11.5	3.42	2.8	AH11	9.8	1.60	2.7
AH83	12.5	1.29	1.9	AH29	11.2	1.42	1.0
AH4	9.4	0.23	0.4	AH56	9.6	1.80	0.9
AH6	9.1	0.56	0.7	AH13	12.3	2.25	1.3
AH117	12.9	1.83	2.0	AH38	10.9	1.70	1.0

(b)

Sample	P (kbar)	sd (kbar)	sigfit
AH6	16.2	3.45	1.0
AH117	21.3	2.72	1.2
AH7	22.2	2.38	0.1
AH9	18.1	2.84	0.9
AH11	23.9	2.49	0.1
AH29	18.6	3.58	1.1
AH13	17.5	4.06	1.3

Table 4: (a) Results of P calculations using the full inferred equilibrium assemblage and an assumed formation temperature of 650 °C. (b) Results of P calculations with the assemblage g + mu + ky + q for an assumed formation temperature of 700 °C.

gradient of about 1.3 kbar / 10 km (Fig. 5). This gradient is a minimum estimate, because the transect line is not normal to the metamorphic isograds, the orientation of which is not exactly known. However, the derived gradient is consistent with metamorphic pressure data from the southern Koralpe (Tenczer and Stüwe, 2003) (Fig. 5, left margin). Moreover, extrapolation of this gradient to the north results in pressures around 10 kbar some 50 km north of the Plankogel detachment, consistent with the metamorphic pressures of the Gleinalpe complex (Neubauer et al., 1995). To the south, this gradient may be extrapolated into the SBUC where there is a debate about the magnitude of the peak metamorphic pressures (Janák et al., 2004; Miller and Konzett, 2005). The finding of diamonds by Janák et al. (2015) suggests pressures of 35 kbar in the SBUC. However, all UHP rocks of the SBUC are located inside the so-called Slovenska Bistrica

antiform, which is interpreted to be an isolated fold structure that formed during the exhumation processes (Kirst et al., 2010). As such, the extremely high pressure of the SBUC rocks do not contradict the extrapolation of the field gradient to the south. This extrapolated field gradient indicates some 22 kbar for the formation pressures in the general region of the SBUC (Fig. 5), supporting the interpretation of Sassi et al. (2004) and Janák et al. (2009).

5.1 Tectonic interpretation

The pressure gradient across the high pressure belt of the Eastern Alps has been interpreted to represent a south- to eastward-dipping subduction zone (e.g. Janák et al., 2004). The Pohorje mountains metamorphic conditions are consistent with this concept since they exhibit very high pressures. Indeed, the metamorphic field gradient inferred here (1.3 kbar/10 km) corresponds to a depth increase of about 0.49 kilometer per kilometer in the field (assuming lithostatic pressure and a density of 2700 kg/m³ for the overlying rocks). While there has been some debate on the influence of non-lithostatic pressures during metamorphism of the Eoalpine high pressure belt (Ehlers et al., 1994), a lithostatic interpretation for the pressures is geometrically elegantly interpreted: It may be seen as evidence for a subduction zone dipping with 45° to the south that was later tilted into a horizontal position due to extraction of a slab in its hanging wall (Fig. 6). The surface of this subducted slab may correspond to the entire transect from the northern Koralpe to the southernmost Pohorje, with the exception of the structural perturbation of the Slovenska Bistrica antiform at the southern end of the transect that formed during the exhumation processes (Kirst et al., 2010). Within this model, the Plattengneis-Plankogel detachment (PGPK shear zone) may be interpreted as the trace of the slab extracted above the subducting plate with the Plankogel Unit representing the hanging wall of the extracted slab (Schorn and Stüwe, 2016) (Fig. 6)

and a second exhumation stage must be invoked to exhume the transect from mid-amphibolite facies conditions to the surface. However, the Plankogel Unit separates the eclogite facies rocks of the Koralpe from the eclogite facies rocks of the Pohorje. This interruption questions the relationship between the high pressure rocks in the Koralpe and the Pohorje and the model of slab extraction in general because it allows two possible interpretations that differ with respect to the structural position of the Plankogel Unit. These two possibilities are difficult to resolve in the field because of Miocene and post-Miocene cover.

The first model suggests that the south-dipping PGPK shear zone as well as the Plankogel Unit continue downwards at depth and separate the Pohorje mountains from the Koralpe. Within this model, the Pohorje mountains could not have been situated in the footwall of the same extracted slab as the Koralpe. This would imply that the Pohorje followed a different tectonic history. Due to the high pressures reported for the SBUC, the high grade rocks in the Pohorje mountains must have been located even deeper within the crust than those in the Koralpe. South of the subduction zone, another tectonic contact could potentially have hosted the rocks of the Pohorje region. In view of the pressure values clearly rising consistently from the Koralpe to the Pohorje, this model is considered to be unlikely.

The second model invokes a vertical offset of the Pohorje relative to the Koralpe due to later processes, for example during normal faulting (Fig. 7). Within this model, the Koralpe and Pohorje rocks both resided in the footwall of the same extracted slab (Fig. 6). For this model, a shear zone system must be invoked that displaces the rocks of the Pohorje mountains and the overlying Plankogel Unit upwards relative to the Koralpe by several kilometers so that the south dipping Plankogel Unit is eroded everywhere south of this fault system (roughly in the Drava valley). This offset must be large enough so that the Plankogel Unit does not re-appear at the southern end of the

Pohorje mountains. Here we suggest that such shearing with normal sense of shear must involve also at least about 10 kilometers of vertical south—side-up offset of the Pohorje relative to the Koralpe causing at least part of the second stage of exhumation.

Invoking normal faulting (Fig. 7) provides an elegant explanation for both the observed relative position of the different lithologies as shown on Fig. 2 and a tectonic process that causes the

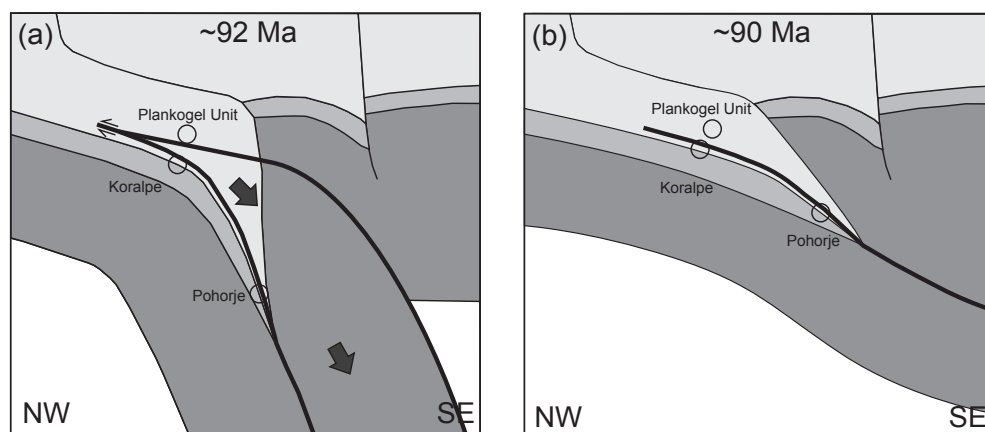


Figure 6: Simplified tectonic sketches of the Eastern Alps during Eoalpine subduction (modified after Schorn and Stüwe, 2016). (a) The sketch shows the positions of the Koralpe, Plankogel Unit and Pohorje in relation to the Eoalpine subduction zone around 92 Ma. (b) The second sketch shows the positions of the Koralpe, Plankogel Unit and Pohorje after the slab extraction around 90 Ma.

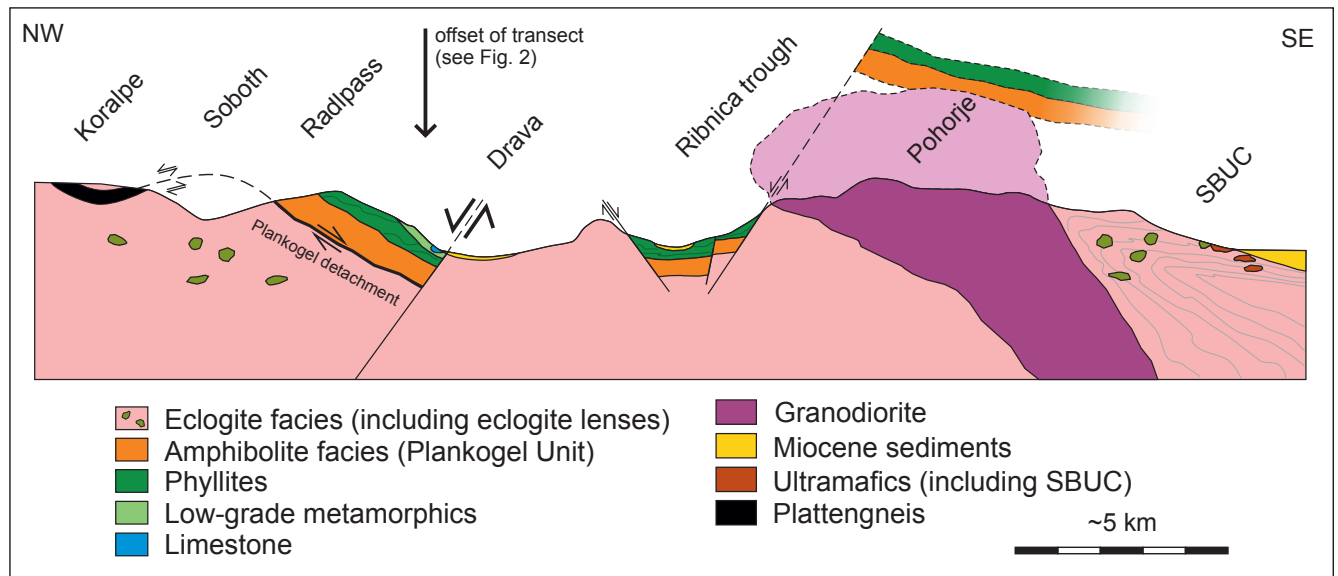


Figure 7: Geological profile through the studied transect as inferred from our metamorphic data and consistent with Fig. 2. The sense of shear for the Plankogel detachment and the Plattengneis are after Schorn and Stüwe (2016). The normal faults near the Drava valley and the Ribnica trough are inferred to be consistent with normal faulting during the 2nd stage of exhumation as suggested by Neubauer (1995) and as seen on the map on Fig. 1. The arrow indicates the location of the jump in the section.

2nd stage of exhumation. Indeed, several authors have suggested that extensional processes played a role during the exhumation of the Koralpe region. For example, Neubauer et al. (1995) has recognized significant late Cretaceous extension processes during exhumation of the Gleinalpe to the north and Fodor et al. (2002) has suggested that east - to north-east-directed low angle extensional shearing is responsible for the exhumation of the Pohorje mountains. Low angle normal faulting in the region is also consistent with the serrated outcrop pattern of different units as shown in Fig. 2. While much of this normal faulting is likely to have occurred during the latest Cretaceous, the final exhumation may have occurred as late as the Early to Middle Miocene as demonstrated by apatite and zircon fission track ages of 19 – 10 Ma and K – Ar mica ages of 19 – 13 Ma from country rocks of eclogites and metaultrabasites (Fodor et al., 2002). Nevertheless, we suggest that the homogeneity of the amphibolite facies metamorphic conditions following the slab extraction process along the (Fig. 5) indicates that final exhumation was mostly driven by erosion driven denudation.

6 Conclusion

In this study, geothermobarometry has been used to constrain the tectonic and metamorphic history of the southern part of the Eastern Alps. In summary, the following can be concluded:

- (i) Pressures to the south of the eclogite facies units of the Koralpe drop within the area of the Plankogel Unit to $7.1 \pm 1.95 - 11.5 \pm 3.42$ kbar at an estimated temperature of 650 °C.
- (ii) In the Pohorje region, pressures for high metamorphic grade metapelites exhibit values from 9.7 ± 2.54 kbar to 12.9 ± 1.83 kbar at 650 °C for decompression

conditions and peak metamorphic pressures that rise from 16.2 ± 3.45 kbar in the north to 23.9 ± 2.49 kbar at 700 °C in the south.

- (iii) The entire Koralpe and Pohorje regions can be fitted with a metamorphic field gradient of about 1.3 kbar per 10 kilometers corresponding to the depth increase of 0.49 km per kilometer along a north-south transect.
- (iv) The good correspondence between the conditions in the northern Pohorje and southern Koralpe suggests that the Koralpe and Pohorje mountains were subducted together during the Eoalpine metamorphic event and subsequently partly exhumed to mid-amphibolite facies conditions due to slab extraction within the subduction zone. The Plattengneis Plankogel shear zone represents the trace of this extraction (Schorn and Stüwe, 2016).
- (v) Exhumation from the mid-amphibolite facies conditions to the surface occurred during a 2nd exhumation stage that is best interpreted as an extensional faulting event. Invoking such an event is consistent with extensional processes as inferred by Neubauer et al. (1995) or Fodor et al. (2002) and the mapped distribution of lithologies in the field.

Acknowledgements

R. Powell, V. Tenczer and R. White are thanked for advice and help on specific questions regarding geothermobarometric calculations. S. Schorn is thanked for constructive comments and help with calculations. R. Schuster is thanked for discussions of the tectonic interpretation of the considered region. P. Schantl is thanked for help with interpreting the mineral analyses. A. Pock is thanked for his assistance during laboratory work. The assistance of K. Ettinger and J. Neubauer at the electron microprobe is

thankfully acknowledged. M. Reiser and an anonymous review are thanked for a series of critical comments and H. Ortner and M. Wagreich for editorial handling of the manuscript.

References

- Eberlei T., Johnson T. E., White R. W., Roffeis C. and Stüwe K., 2014. Thermobarometric constraints on pressure variations across the Plattengneis shear zone of the Eastern Alps: implications for exhumation models during Eoalpine subduction. *Journal of Metamorphic Geology*, 32, 227–244. <https://doi.org/10.1111/jmg.12069>
- Ehlers K., Stüwe K., Powell R., Sandiford M. and Frank W., 1994. Thermometrically inferred cooling rates from the Plattengneis, Koralm region, Eastern Alps Earth and Planetary Science Letters, 125, 307–321.
- Fodor L.I., Jelen B., Márton E., Zupančič N., Trajanova M., Rifelj H., Pécskay Z., Balogh K., Koroknai B., Dunkl I., Horváth P., Horvat A., Vrabec M., Kraljić M. and Kevrić R., 2002. Connection of Neogene basin formation, magmatism and cooling of metamorphics in NE Slovenia. *Geologica Carpathica*, 53, 199–201.
- Fodor L.I., Gerdes A., Dunkl I., Koroknai B., Pécskay Z., Trajanova M., Horváth P., Vrabec M., Jelen B., Balogh K. and Frisch W., 2008. Miocene emplacement and rapid cooling of the Pohorje pluton at the Alpine-Pannonian-Dinaridic junction, Slovenia. *Swiss Journal of Geosciences*, 101, 255–271. <https://doi.org/10.1007/s00015-008-1286-9>
- Froitzheim N., Pleuger J., Roller S. and Nagel T., 2003. Exhumation of high- and ultrahigh-pressure metamorphic rocks by slab extraction. *Geology*, 31, 925–928. <https://doi.org/10.1130/G19748.1>
- Froitzheim N., Pleuger J. and Nagel T., 2006. Extraction faults. *Journal of Structural Geology*, 28, 1388–1395. <https://doi.org/10.1016/j.jsg.2006.05.002>
- Froitzheim N., Plašienka D. and Schuster R., 2008. Alpine tectonics of the Alps and Western Carpathians. In: McCann, T. (Ed.): *The Geology of Central Europe. Volume 2: Mesozoic and Cenozoic*. Geological Society of London, 1141–1232.
- Gregurek D., Abart R. and Hoinkes G., 1997. Contrasting Eoalpine P-T evolutions in the southern Koralpe, Eastern Alps. *Mineralogy and Petrology*, 60, 61–80. <https://doi.org/10.1007/BF01163135>
- Hinterlechner-Ravnik A., 1977. Geochemical Characteristics of the Metamorphic Rocks of the Pohorje Mountains. *Geologija*, 20, 107–140.
- Hoinkes G., Koller F., Ranitsch G., Dachs E., Höck V., Neubauer F. and Schuster R., 1999. Alpine metamorphism of the Eastern Alps. *Schweizerische Mineralogische und Petrographische Mitteilungen*, 79, 155–181.
- Holland T.J.B. and Powell R., 1998. An internally consistent thermodynamic data set for phases of petrological interest. *Journal of Metamorphic Geology*, 16, 309–343. <https://doi.org/10.1111/j.1525-1314.1998.00140.x>
- De Hoog J.C.M., Janák M., Vrabec M. and Froitzheim N., 2009. Serpentinised peridotites from an ultrahigh-pressure terrane in the Pohorje Mts. (Eastern Alps, Slovenia): Geochemical constraints on petrogenesis and tectonic setting. *Lithos*, 109, 209–222. <https://doi.org/10.1016/j.lithos.2008.05.006>
- Hurai V., Janák M. and Thomas R., 2010. Fluid-assisted retrogression of garnet and P–T history of metapelites from HP/UHP metamorphic terrane (Pohorje Mountains, Eastern Alps). *Contributions to Mineralogy and Petrology*, 160, 203–218. <https://doi.org/10.1007/s00410-009-0473-7>
- Janák M., Froitzheim N., Lupták B., Vrabec M. and Krogh Ravna E.J., 2004. First evidence for ultrahigh-pressure metamorphism of eclogites in Pohorje, Slovenia: Tracing deep continental subduction in the Eastern Alps. *Tectonics*, 23, TC5014. <https://doi.org/10.1029/2004TC001641>
- Janák M., Froitzheim N., Vrabec M. and Krogh Ravna E.J., 2005. Reply to comment by C. Miller and J. Konzett on “First evidence for ultrahigh-pressure metamorphism of eclogites in Pohorje, Slovenia: Tracing deep continental subduction in the eastern Alps”. *Tectonics*, 24, TC6011. <https://doi.org/10.1029/2005TC001875>
- Janák M., Froitzheim N., Vrabec M., Krogh Ravna E.J. and De Hoog J.C.M., 2006. Ultrahigh-pressure metamorphism and exhumation of garnet peridotite in Pohorje, Eastern Alps. *Journal of Metamorphic Geology*, 24, 19–31. <https://doi.org/10.1111/j.1525-1314.2005.00619.x>
- Janák M., Cornell D., Froitzheim N., De Hoog J.C.M., Broska I., Vrabec M. and Hurai V., 2009. Eclogite-hosting metapelites from the Pohorje Mountains (Eastern Alps): P–T evolution, zircon geochronology and tectonic implications. *European Journal of Mineralogy*, 21, 1191–1212. <https://doi.org/10.1127/0935-1221/2009/0021-1966>
- Janák M., Froitzheim N., Yoshida K., Sasinková V., Nosko M., Kobayashi T., Hirajima T. and Vrabec M., 2015. Diamond in metasedimentary crustal rocks from Pohorje, Eastern Alps: a window to deep continental subduction. *Journal of Metamorphic Geology*, 33, 495–512. <https://doi.org/10.1111/jmg.12130>
- Kirst F., Sandmann S., Nagel T.J., Froitzheim N. and Janák M., 2010. Tectonic evolution of the southeastern part of the Pohorje Mountains (Eastern Alps, Slovenia). *Geologica Carpathica*, 61, 6, 451–461. <https://doi.org/10.2478/v10096-010-0027-y>
- Kleinschmidt G., 1975. Die „Plankogelserie“ in der südlichen Koralpe unter besonderer Berücksichtigung von Manganquarziten. *Verhandlungen der Geologischen Bundesanstalt*, 2–3, 351–362.
- Kurz W., Fritz H., Tenczer V. and Unzog W., 2002. Tectonometamorphic evolution of the Koralm Complex (Eastern Alps): constraints from microstructures and textures of the ‘Plattengneis’ shear zone. *Journal of Structural Geology*, 24, 1957–1970. [https://doi.org/10.1016/S0191-8141\(02\)00008-1](https://doi.org/10.1016/S0191-8141(02)00008-1)
- Miller C. and Thöni M., 1997. Eo-Alpine eclogitisation of Permian MORB-type gabbros in the Koralpe (Eastern

- Alps, Austria): new geochronological, geochemical and petrological data. *Chemical Geology*, 137, 283–310. [https://doi.org/10.1016/S0009-2541\(96\)00165-9](https://doi.org/10.1016/S0009-2541(96)00165-9)
- Miller C. and Konzett J., 2005. Comment on “First evidence for ultrahigh-pressure metamorphism of eclogites in Pohorje, Slovenia: Tracing deep continental subduction in the eastern Alps” by Marian Janák et al. *Tectonics*, 24, TC6010. <https://doi.org/10.1029/2004TC001765>
- Miller C., Mundil R., Thöni M. and Konzett J., 2005. Refining the timing of eclogite metamorphism: a geochemical, petrological, Sm-Nd and U-Pb case study from the Pohorje Mountains, Slovenia (Eastern Alps). *Contributions to Mineralogy and Petrology*, 150, 70–84. <https://doi.org/10.1007/s00410-005-0004-0>
- Miller C., Zanetti A., Thöni M. and Konzett J., 2007. Eclogitisation of gabbroic rocks: Redistribution of trace elements and Zr in rutile thermometry in an Eo-Alpine subduction zone (Eastern Alps). *Chemical Geology*, 239, 96–123. <https://doi.org/10.1016/j.chemgeo.2007.01.001>
- Mioč P. and Žnidarčič M., 1977. Geological map of SFRJ 1:100 000, Sheet Slovenj Gradec. Geological Survey, Ljubljana, Federal Geological Survey, Beograd.
- Neubauer F., Dallmeyer R.D., Dunkl I. and Schirnik D., 1995. Late Cretaceous exhumation of the metamorphic Gleinalm dome, Eastern Alps: kinematics, cooling history and sedimentary response in a sinistral wrench corridor. *Tectonophysics*, 242, 79–98. [https://doi.org/10.1016/0040-1951\(94\)00154-2](https://doi.org/10.1016/0040-1951(94)00154-2)
- Neugebauer J., 1970. Alt-paläozoische Schichtfolge, Deckenbau und Metamorphose-Ablauf im südwestlichen Saualpen-Kristallin (Ostalpen). *Geotektonische Forschungen*, 35, 23–93.
- Powell R. and Holland T.J.B., 1988. An internally consistent dataset with uncertainties and correlations: 3. Applications to geobarometry, worked examples and a computer program. *Journal of Metamorphic Geology*, 6, 173–204. <https://doi.org/10.1111/j.1525-1314.1988.tb00415.x>
- Powell R. and Holland T.J.B., 1994. Optimal geothermometry and geobarometry. *American Mineralogist*, 79, 120–133.
- Sandmann S., Herwartz D., Kirst F., Froitzheim N., Nagel T., Fonseca R., Münker C. and Janák M., 2016. Timing of eclogite-facies metamorphism of mafic and ultramafic rocks from the Pohorje Mountains (Eastern Alps, Slovenia) based on Lu-Hf garnet geochronometry. *Lithos*, 262, 576–585. <https://doi.org/10.1016/j.lithos.2016.08.002>
- Sassi R., Mazzoli C., Miller C. and Konzett J., 2004. Geochemistry and metamorphic evolution of the Pohorje Mountain eclogites from the easternmost Austroalpine basement of the Eastern Alps (Northern Slovenia). *Lithos*, 78, 235–261. <https://doi.org/10.1016/j.lithos.2004.05.002>
- Schmid S.M., Fügenschuh B., Kissling E. and Schuster R., 2004. Tectonic map and overall architecture of the Alpine orogen. *Eclogae Geologicae Helvetiae*, 97, 93–117. <https://doi.org/10.1007/s00015-004-1113-x>
- Schorn S. and Stüwe K., 2016. The Plankogel detachment of the Eastern Alps: petrological evidence for an orogen-scale extraction fault. *Journal of Metamorphic Geology*, 34, 147–166. <https://doi.org/10.1111/jmg.12176>
- Schuster R., 2003. Das eo-Alpidische Ereignis in den Ostalpen: Plattentektonische Situation und interne Struktur des Ostalpinen Kristallins. Arbeitstagung 2003 der Geologischen Bundesanstalt, Blatt 148 Brenner, 141–159.
- Schuster R. and Stüwe K., 2008. Permian metamorphic event in the Alps. *Geology*, 36, 963–966.
- Stüwe K. and Schuster R., 2010. Initiation of subduction in the Alps: Continent or ocean? *Geology*, 38, 175–178. <https://doi.org/10.1130/G30528.1>
- Tenczer V. and Stüwe K., 2003. The metamorphic field gradient in the eclogite type locality, Koralpe region, Eastern Alps. *Journal of Metamorphic Geology*, 21, 377–393. <https://doi.org/10.1046/j.1525-1314.2003.00448.x>
- Tenczer V., Powell R. and Stüwe K., 2006. Evolution of H₂O content in a polymetamorphic terrane: the Plattengneis Shear Zone (Koralpe, Austria). *Journal of Metamorphic Geology*, 24, 281–295. <https://doi.org/10.1111/j.1525-1314.2006.00637.x>
- Thöni M., 2002. Sm–Nd isotope systematics in garnet from different lithologies (Eastern Alps): age results and an evaluation of potential problems for garnet Sm–Nd chronometry. *Chemical Geology*, 185, 255–281. [https://doi.org/10.1016/S0009-2541\(02\)00419-9](https://doi.org/10.1016/S0009-2541(02)00419-9)
- Thöni M., 2006. Dating eclogites-facies metamorphism in the Eastern Alps – approaches, results, interpretations: a review. *Mineralogy and Petrology*, 88, 123–148. <https://doi.org/10.1007/s00710-006-0153-5>
- Thöni M. and Jagoutz E., 1992. Some new aspects of dating eclogites in orogenic belts: Sm–Nd, Rb–Sr, and Pb–Pb isotopic results from the Austroalpine Saualpe and Koralpe type-locality (Carinthia/Styria, southeastern Austria). *Geochimica et Cosmochimica Acta*, 56, 347–368. [https://doi.org/10.1016/0016-7037\(92\)90138-9](https://doi.org/10.1016/0016-7037(92)90138-9)
- Thöni M. and Jagoutz E., 1993. Isotopic constraints for Eoalpine high-P metamorphism in the Austroalpine Nappes of the Eastern Alps: bearing on Alpine orogenesis. *Schweizerische Mineralogische und Petrographische Mitteilungen*, 73, 177–189.
- Thöni M. and Miller C., 1996. Garnet Sm–Nd data from the Saualpe and the Koralpe (Eastern Alps, Austria): chronological and P–T constraints on the thermal and tectonic history. *Journal of Metamorphic Geology*, 14, 453–466. <https://doi.org/10.1046/j.1525-1314.1996.05995.x>
- Thöni M. and Miller C., 2009. The “Permian event” in the Eastern European Alps: Sm–Nd and P–T data recorded by multi-stage garnet from the Plankogel unit. *Chemical Geology*, 260, 20–36. <https://doi.org/10.1016/j.chemgeo.2008.11.017>
- Thöni M., Miller C., Blichert-Toft J., Whitehouse M.J., Konzett J. and Zanetti A., 2008. Timing of high-pressure metamorphism and exhumation of the eclogite type-locality (Kupplerbrunn–Prickler Halt, Saualpe, south-eastern Austria): constraints from correlations of the Sm–Nd, Lu–Hf, U–Pb and Rb–Sr isotopic systems.

- Journal of Metamorphic Geology, 26, 561–581. <https://doi.org/10.1111/j.1525-1314.2008.00778.x>
- Trajanova M., Pécskay Z. and Itaya T., 2008. K-Ar geochronology and petrography of the Miocene Pohorje Mountains batholith (Slovenia). *Geologica Carpathica*, 59, 3, 247–260.
- Vrabec M., Janák M., Froitzheim N. and De Hoog J.C.M., 2012. Phase relations during peak metamorphism and decompression of the UHP kyanite eclogites, Pohorje Mountains (Eastern Alps, Slovenia). *Lithos*, 144–145, 40–55. <https://doi.org/10.1016/j.lithos.2012.04.004>
- Wiesinger M., Neubauer F. and Handler R., 2006. Exhumation of the Saualpe eclogite Unit, Eastern Alps: constraints from $^{40}\text{Ar}/^{39}\text{Ar}$ ages and structural investigations. *Mineralogy and Petrology*, 88, 149–180. <https://doi.org/10.1007/s00710-006-0154-4>

Submitted: 10 04 2018

Accepted: 13 08 2018

Alexandra HERG^{*)} & Kurt STÜWE

Institute of Earth Sciences, University of Graz, Universitätsplatz 2, A-8010, Graz, Austria;

^{*)}Corresponding author: Alexandra Herg, alexandra@m-herg.at

SUPPLEMENTARY

Sample	AH87					
	garnet					
Mineral	rim		core		core	
Position	rim	rim	rim	core	core	core
SiO ₂	37.62	38.11	37.71	36.21	36.99	36.89
TiO ₂	0.03	0.00	0.02	0.00	0.00	0.00
Al ₂ O ₃	20.52	21.16	20.46	20.37	20.30	20.69
Cr ₂ O ₃	0.06	0.02	0.00	0.05	0.00	0.03
Fe ₂ O ₃	0.86	0.15	0.00	1.47	1.78	1.71
FeO	32.87	33.37	33.78	37.92	36.31	37.70
MnO	0.00	0.10	0.05	1.03	1.01	0.77
MgO	3.37	2.98	2.88	1.51	2.18	2.02
CaO	4.72	5.19	4.48	1.28	2.20	1.50
Na ₂ O	0.00	0.01	0.00	0.00	0.00	0.00
K ₂ O	0.03	0.02	0.00	0.00	0.06	0.03
Total	100.07	101.11	99.38	99.85	100.84	101.36
Oxygen	12.0	12.0	12.0	12.0	12.0	12.0
Si	3.006	3.012	3.037	2.969	2.984	2.968
Ti	0.002	0.000	0.001	0.000	0.000	0.000
Al	1.933	1.971	1.943	1.969	1.931	1.962
Cr	0.004	0.001	0.000	0.004	0.000	0.002
Fe ³⁺	0.052	0.009	0.000	0.091	0.108	0.104
Fe ²⁺	2.196	2.206	2.275	2.600	2.449	2.537
Mn	0.000	0.007	0.003	0.071	0.069	0.052
Mg	0.401	0.351	0.346	0.185	0.263	0.243
Ca	0.404	0.440	0.387	0.113	0.190	0.129
Na	0.000	0.002	0.000	0.000	0.000	0.001
K	0.003	0.002	0.000	0.000	0.006	0.003
Total	8.000	8.000	7.991	8.000	8.000	8.000

Table S1: Representative garnet compositions for samples from the Plankogel Unit.